Probe of Spin Dynamics in Superconducting NbN Thin Films via Spin Pumping

Yunyan Yao^{1,2}, Qi Song^{1,2}, Yota Takamura^{3,4}, Juan Pedro Cascales³, Wei Yuan^{1,2}, Yang Ma^{1,2}, Yu Yun^{1,2}, Jagadeesh S. Moodera^{3,5}, X. C. Xie^{1,2}, and Wei Han^{1,2*}

¹ International Center for Quantum Materials, School of Physics, Peking University, Beijing 100871, P. R. China

² Collaborative Innovation Center of Quantum Matter, Beijing 100871, P. R. China

³ Plasma Science and Fusion Center and Francis Bitter Magnet Laboratory, Massachusetts Institute of Technology, Cambridge, MA 02139, USA

⁴ School of Engineering, Tokyo Institute of Technology, Tokyo 152-8550, Japan

⁵ Department of Physics, Massachusetts Institute of Technology, Cambridge, MA 02139, USA

* Correspondence to: weihan@pku.edu.cn (W.H.)

The emerging field of superconductor (SC) spintronics has attracted intensive attentions recently¹⁻³. Many fantastic spin dependent properties in SC have been discovered, including the observation of large magnetoresistance, long spin lifetimes and the giant spin Hall effect in SC, as well as spin supercurrent in Josephson junctions, etc⁴⁻¹⁰. Regarding the spin dynamic in SC films, few studies has been reported yet. Here, we report the investigation of the spin dynamics in an s-wave superconducting NbN film via spin pumping from an

adjacent insulating ferromagnet GdN layer. A profound coherence peak of the Gilbert damping is observed slightly below the superconducting critical temperature of the NbN layer, which is consistent with recent theoretical studies¹¹. Our results further indicate that spin pumping could be a powerful tool for investigating the spin dynamics in 2D crystalline superconductors¹².

The spin susceptibility is one of the most important physical properties of a SC. The Messier-Oschenfeld effect refers to the sudden decrease of the static spin susceptibility, which is one of the two essential hall marks for superconductivity¹³. Regarding the dynamic spin susceptibility, previous studies have been focused on bulk SCs, by measuring the spin-lattice relaxation rate via nuclear magnetic resonance technique¹³⁻¹⁵. It also provides an avenue for identifying unconventional superconducting paring mechanisms¹⁶, while limited to mostly bulk SCs due to low signal-to-noise ratio. The recent discovery of interfacial and two-dimensional SCs presents an emerging research direction to investigate their dynamic spin susceptibility^{12,17,18}.

A recent theoretical study shows the possibility for observing the spin dynamics in superconducting films via spin pumping¹¹, a well-established technique to enable spin injection and to probe the dynamic spin susceptibility in various materials, including metal, semiconductors, Rashba 2DEGs, and topological insulators, etc¹⁹⁻²⁸. Here, we report the experimental investigation of the spin dynamics in s-wave superconducting NbN thin films via spin pumping from an insulating ferromagnet (FM) GdN layer using trilayers of NbN/GdN/NbN.

Figure 1a illustrates the spin pumping with the interfacial *s-d* exchange coupling between the Cooper pairs in the NbN layer and the magnetic moment in the GdN layer, which gives rise to an

additional Gilbert damping to that of the GdN layer under the magnetization resonance conditions. NbN is an s-wave SC with a superconducting coherence length of ~ 5 nm and a spin diffusion length of ~ 7 nm⁸. The Gilbert damping of the GdN in the NbN (t)/GdN (d)/NbN (t) trilayer heterostructures is measured via ferromagnetic resonance (FMR) technique (see Methods for details). In a typical sample consisting of NbN (10)/GdN (5)/NbN (10), with thickness in nm, the Curie temperature (T_{Curie}) of GdN is determined to be ~ 38 K (Fig. 1b), and the superconducting critical temperature (T_{C}) of NbN is ~ 10.8 K (Fig. 1c) (see Methods for details). Fig. 1d shows a typical FMR signal (S_{21}) vs. the magnetic field of this sample at 10 K, with a microwave excitation frequency (f) of 15 GHz. The half linewidth (ΔH) could be obtained by the Lorentz fitting of the signal:

$$S_{21} \propto S_0 \frac{(\Delta H)^2}{(\Delta H)^2 + (H - H_{pos})^2}$$
 (1)

where S_0 is the constant describing the coefficient for the transmitted microwave power, H is the external magnetic field, and H_{res} is the resonance magnetic field. Gilbert damping (α) is determined using numerical fitting of ΔH at various frequencies (Fig. 1e) by taking into account a temperature-dependent spin-relaxation time constant (τ)(Supplementary Information S1)²⁹:

$$\Delta H = \Delta H_0 + \frac{4\pi\alpha f}{\gamma} + A \frac{2\pi f \tau}{1 + (2\pi f \tau)^2} \tag{2}$$

where ΔH_0 is related to the inhomogeneous properties, γ is the gyromagnetic ratio, and A is the spin relaxation coefficient.

The Gilbert damping is investigated as a function of the temperature for two trilayer samples of NbN (2)/GdN (5)/NbN (2) and NbN (10)/GdN (5)/NbN (10) which exhibit different T_C (Fig. 2a). Interestingly, a profound coherence peak of the Gilbert damping in the NbN (10)/GdN (5)/NbN (10) is observed, as shown in Fig. 2b. Whileas, a contrasting behavior of the Gilbert damping in the NbN (2)/GdN (5)/NbN (2) is observed, which exhibits a monotonic decrease as the temperature decreases down to 6 K. The peak of the Gilbert damping in the NbN (10)/GdN (5)/NbN (10) is observed at \sim 8.5 K, which is slightly below the T_C (\sim 10.7 K) of the 10 nm NbN layer. These results indicate the successful dynamic spin injection into the 10 nm NbN layer, which authenticates a charge-free method to inject spin-polarized carriers into a SC beyond previous reports of electrical spin injections^{6,7,30,31}. Furthermore, the observation of the profound coherence peak below the T_C is exactly expected by recent theoretical calculations of the spin dynamics in an s-wave SC¹¹. In their theory, the Gilbert damping is related to the interfacial *s-d* exchange interaction and the imaginary part of the dynamic spin susceptibility of the SC.

$$\delta \alpha \propto J_{sd}^2 \sum_q \operatorname{Im} x_q^R(\varpi)$$
 (3)

For the s-wave superconducting NbN thin films, the superconducting gap Δ opens at the Fermi level below the T_C . At the temperature slightly below T_C , two coherence peaks of the density states exist around the edge of the superconducting gap following the BCS theory¹³, and these peaks in turn give rise to the enhancement of the dynamic spin susceptibility.

The enhancement of the dynamic spin susceptibility is also evidenced by the temperature dependent spin-lattice relaxation rate of bulk s-wave SCs, which has been considered as one of the important experimental evidences of the well-known BCS theory¹³⁻¹⁵. As the temperature further decreases, the number of quasiparticles decreases as the Δ grows, thereby the Gilbert damping

decreases as the temperature falls below 8 K. Noteworthy is that our results are essentially different from previous reports of spin pumping into SC Nb films using the ferromagnetic metal permalloy, where a monotonic decrease of the Gilbert damping is reported when the temperature decreases^{32,33}. In their experiment, as permalloy is a metal, the interface behavior is expected to be different⁵. However, in the present study, a FM insulating GdN is used, charge carriers from NbN do not penetrate into GdN, thus not weakening the SC at the interface and so that the superconducting gap survives^{34,35}.

Next, the thickness of the GdN layer is varied to further study the interface proximity effect and the spin dynamics in NbN layer. For all these samples consisting of NbN (10)/GdN (d)/NbN (10) with d from 10 to 30 nm, a profound coherence peak of the Gilbert damping is observed slightly below the superconducting temperature of NbN, as shown in Figs. 3a and 3b (red circles). While for all the samples consisting of NbN (2)/GdN (d)/NbN (2), no such coherence peak of the Gilbert damping is noticeable (green circles in Figs. 3a and 3b). The role of the effective magnetization has been ruled out since it exhibits similar temperature dependence for NbN (2)/GdN (5)/NbN (2) and NbN (10)/GdN (5)/NbN (10) samples (Supplementary Information S2). As the enhanced Gilbert damping is an interface effect, the coherence peak is less conspicuous when the GdN film is thicker. The ratio of the peak Gilbert damping constant over the value at T_C is plotted as a function of the GdN thickness (Fig. 3c), given that samples NbN (10)/GdN (d)/NbN (10) show a similar Tc (Supplementary Fig. S4). For a deeper understanding of the underlying mechanism further studies is needed. One possible cause might be related to the interface proximity exchange effect and/or presence of magnetic loose spins leading to scattering at the interface, which could affect the spin diffusion length and coherence length of the NbN layer.

To further confirm the observed coherence peak of the Gilbert damping is an interface effect arising from the s-d exchange interaction, the Gilbert damping at each temperature is plotted as a function of the thickness of the GdN layer (Fig. 4a). The interface-induced Gilbert damping could be estimated based on the thickness dependence of the total Gilbert damping (Supplementary Information S3), since a similar T_C is observed in all the samples NbN (10)/GdN (d)/NbN (10). The unperturbed peak at ~ 8.5 K (Fig. 4b) unambiguously demonstrates that the origin of the coherence peak in the Gilbert damping is indeed due to the interfacial s-d exchange interaction between the magnetization of GdN and the spins in the Cooper pairs of NbN in its superconducting state. For comparison, the interface-induced Gilbert damping in the samples of NbN (2)/GdN (d)/NbN (2) does not show any features of coherence peak at ~ 8.5 K (Supplementary Fig. S5).

In conclusion, the dynamic spin dynamic spin susceptibility of s-wave SC NbN film is investigated via spin pumping from a FM insulating GdN layer. A profound coherence peak of the Gilbert damping is observed below T_C , which strongly corroborates with dynamic spin injection into the SC and the dynamic spin susceptibility in it. Our results could be important for future investigation of the antiferromagnetic fluctuations in unconventional superconducting films, and the spin dynamics of two dimensional and interfacial SC^{12} .

Methods

Films growth

The NbN (t)/GdN (d)/NbN (t) trilayer samples were grown on Al₂O₃ (~5 nm)-buffered thermally oxidized Si substrates by d.c. reactive magnetron sputtering at 300 °C in an ultrahigh vacuum chamber. The NbN layers were deposited from a pure Nb target (99.95%) in Ar and N₂

gas mixture at a pressure of 2.3 mTorr (20% N_2). The GdN films were deposited from a pure Gd target (99.9%) in Ar and N_2 gas mixture at a pressure of 2.8 mTorr (6% N_2). The NbN and GdN layers were of textured crystalline quality with a preferred direction along (111)-orientation, as evidenced by X-ray diffraction θ -2 θ scans (Supplementary Information S4). After the growth, a thin Al_2O_3 layer (~ 10 nm) was deposited *in situ* as a capping layer to avoid sample degradation with air exposure.

Ferromagnetic resonance measurement

The FMR spectra of the multilayer samples were measured using the coplanar wave guide technique with a vector network analyzer (VNA, Agilent E5071C) in the variable temperature insert of a Physical Properties Measurement System (PPMS; Quantum Design). The samples were attached to the coplanar wave guide using insulating silicon paste. During the measurement, the amplitudes of forward complex transmission coefficients (S_{21}) are recorded as a function of the magnetic field from ~ 5000 to 0 Oe at various temperatures for different microwave frequencies.

Critical temperatures measurement

The Curie temperature of the GdN film was determined via the offset-magnetization as a function of the temperature using a Magnetic Properties Measurement System (MPMS; Quantum Design). The T_C of the SC NbN thin films was measured by four-probe resistance technique as a function of the temperature in a Physical Properties Measurement System (PPMS; Quantum Design) using standard ac lock-in technique at low frequency of 7 Hz.

Acknowledgement

We acknowledge the fruitful discussion with Yuan Li and Tao Wu. Y.Y., Q.S., W.Y., Y.M., X.C.X., and W.H. acknowledge the financial support from National Basic Research Programs of China (973 program Grant Nos. 2015CB921104 and 2014CB920902) and National Natural Science Foundation of China (NSFC Grant No. 11574006). Y.T., J.P.C, and J.S.M. acknowledge the grants NSF DMR-1700137 and ONR N00014-16-1-2657. Y.T. also acknowledges the JSPS Overseas Research Fellowships.

Author contributions

W.H. proposed and supervised the project. Y.Y. and Q.S. performed the ferromagnetic resonance measurements. Y.Y. did the electrical transport and the X-ray diffraction measurements. Y.T., J.P.C. and J.S.M. grew the samples. Y.Y. and W.H. analyzed the results. W.H. wrote the manuscript with contributions from all authors.

Competing financial interests

The authors declare no competing financial interests.

References:

- Buzdin, A. I. Proximity effects in superconductor-ferromagnet heterostructures. *Rev. Mod. Phys.* 77, 935-976, (2005).
- Linder, J. & Robinson, J. W. A. Superconducting spintronics. *Nat. Phys.* **11**, 307-315, (2015).
- 3 Eschrig, M. Spin-polarized supercurrents for spintronics. *Phys. Today* **64**, 43-49, (2011).
- Miao, G.-X., Yoon, K., Santos, T. S. & Moodera, J. S. Influence of Spin-Polarized Current on Superconductivity and the Realization of Large Magnetoresistance. *Phys. Rev. Lett.* **98**, 267001, (2007).

- Miao, G.-X., Ramos, A. V. & Moodera, J. S. Infinite Magnetoresistance from the Spin Dependent Proximity Effect in Symmetry Driven bcc-Fe/V/Fe Heteroepitaxial Superconducting Spin Valves. *Phys. Rev. Lett.* **101**, 137001, (2008).
- Yang, H., Yang, S.-H., Takahashi, S., Maekawa, S. & Parkin, S. S. P. Extremely long quasiparticle spin lifetimes in superconducting aluminium using MgO tunnel spin injectors. *Nat. Mater.* **9**, 586-593, (2010).
- Wakamura, T., Hasegawa, N., Ohnishi, K., Niimi, Y. & Otani, Y. Spin Injection into a Superconductor with Strong Spin-Orbit Coupling. *Phys. Rev. Lett.* **112**, 036602, (2014).
- Wakamura, T. *et al.* Quasiparticle-mediated spin Hall effect in a superconductor. *Nat. Mater.* **14**, 675-678, (2015).
- 9 Senapati, K., Blamire, M. G. & Barber, Z. H. Spin-filter Josephson junctions. *Nat. Mater.* **10**, 849-852, (2011).
- Robinson, J. W. A., Witt, J. D. S. & Blamire, M. G. Controlled Injection of Spin-Triplet Supercurrents into a Strong Ferromagnet. *Science* **329**, 59, (2010).
- Inoue, M., Ichioka, M. & Adachi, H. Spin pumping into superconductors: A new probe of spin dynamics in a superconducting thin film. *Phys. Rev. B* **96**, 024414, (2017).
- Saito, Y., Nojima, T. & Iwasa, Y. Highly crystalline 2D superconductors. *Nat. Rev. Mater.* **2**, 16094, (2016).
- 13 Tinkham, M. *Introduction to superconductivity*. (Dover Publications, 2004).
- Masuda, Y. & Redfield, A. G. Nuclear Spin-Lattice Relaxation in Superconducting Aluminum. *Phys. Rev.* **125**, 159-163, (1962).
- Hebel, L. C. & Slichter, C. P. Nuclear Spin Relaxation in Normal and Superconducting Aluminum. *Phys. Rev.* **113**, 1504-1519, (1959).
- 16 Curro, N. J. *et al.* Unconventional superconductivity in PuCoGa5. *Nature* **434**, 622-625, (2005).
- Reyren, N. *et al.* Superconducting Interfaces Between Insulating Oxides. *Science* **317**, 1196-1199, (2007).
- He, S. *et al.* Phase diagram and electronic indication of high-temperature superconductivity at 65 K in single-layer FeSe films. *Nat. Mater.* **12**, 605-610, (2013).
- Tserkovnyak, Y., Brataas, A., Bauer, G. E. W. & Halperin, B. I. Nonlocal magnetization dynamics in ferromagnetic heterostructures. *Rev. Mod. Phys.* 77, 1375-1421, (2005).
- Ohnuma, Y., Adachi, H., Saitoh, E. & Maekawa, S. Enhanced dc spin pumping into a fluctuating ferromagnet near T_C. *Phys. Rev. B* **89**, 174417, (2014).
- Ando, K. *et al.* Inverse spin-Hall effect induced by spin pumping in metallic system. *J. Appl. Phys.* **109**, 103913, (2011).
- Ando, K. *et al.* Electrically tunable spin injector free from the impedance mismatch problem. *Nat. Mater.* **10**, 655-659, (2011).
- Shiomi, Y. *et al.* Spin-Electricity Conversion Induced by Spin Injection into Topological Insulators. *Phys. Rev. Lett.* **113**, 196601, (2014).

- Sánchez, J. C. R. *et al.* Spin-to-charge conversion using Rashba coupling at the interface between non-magnetic materials. *Nat. Commun.* **4**, (2013).
- Song, Q. *et al.* Spin injection and inverse Edelstein effect in the surface states of topological Kondo insulator SmB6. *Nat. Commun.* **7**, 13485, (2016).
- Lesne, E. *et al.* Highly efficient and tunable spin-to-charge conversion through Rashba coupling at oxide interfaces. *Nat. Mater.* **15**, 1261-1266, (2016).
- Song, Q. *et al.* Observation of inverse Edelstein effect in Rashba-split 2DEG between SrTiO3 and LaAlO3 at room temperature. *Science Advances* **3**, e1602312, (2017).
- Ohshima, R. *et al.* Realization of d-electron spin transport at room temperature at a LaAlO3/SrTiO3 interface. *Nat. Mater.* **16**, 609-614, (2017).
- Jermain, C. L. *et al.* Increased low-temperature damping in yttrium iron garnet thin films. *Phys. Rev. B* **95**, 174411, (2017).
- Quay, C. H. L., Chevallier, D., Bena, C. & Aprili, M. Spin imbalance and spin-charge separation in a mesoscopic superconductor. *Nat. Phys.* **9**, 84-88, (2013).
- Hübler, F., Wolf, M. J., Beckmann, D. & v. Löhneysen, H. Long-Range Spin-Polarized Quasiparticle Transport in Mesoscopic Al Superconductors with a Zeeman Splitting. *Phys. Rev. Lett.* **109**, 207001, (2012).
- Bell, C., Milikisyants, S., Huber, M. & Aarts, J. Spin Dynamics in a Superconductor-Ferromagnet Proximity System. *Phys. Rev. Lett.* **100**, 047002, (2008).
- Morten, J. P., Brataas, A., Bauer, G. E. W., Belzig, W. & Tserkovnyak, Y. Proximity-effect–assisted decay of spin currents in superconductors. *Europhys. Lett.* **84**, 57008, (2008).
- De Gennes, P. G. Coupling between ferromagnets through a superconducting layer. *Phys. Lett.* **23**, 10-11, (1966).
- Li, B. *et al.* Superconducting Spin Switch with Infinite Magnetoresistance Induced by an Internal Exchange Field. *Phys. Rev. Lett.* **110**, 097001, (2013).

Figure 1

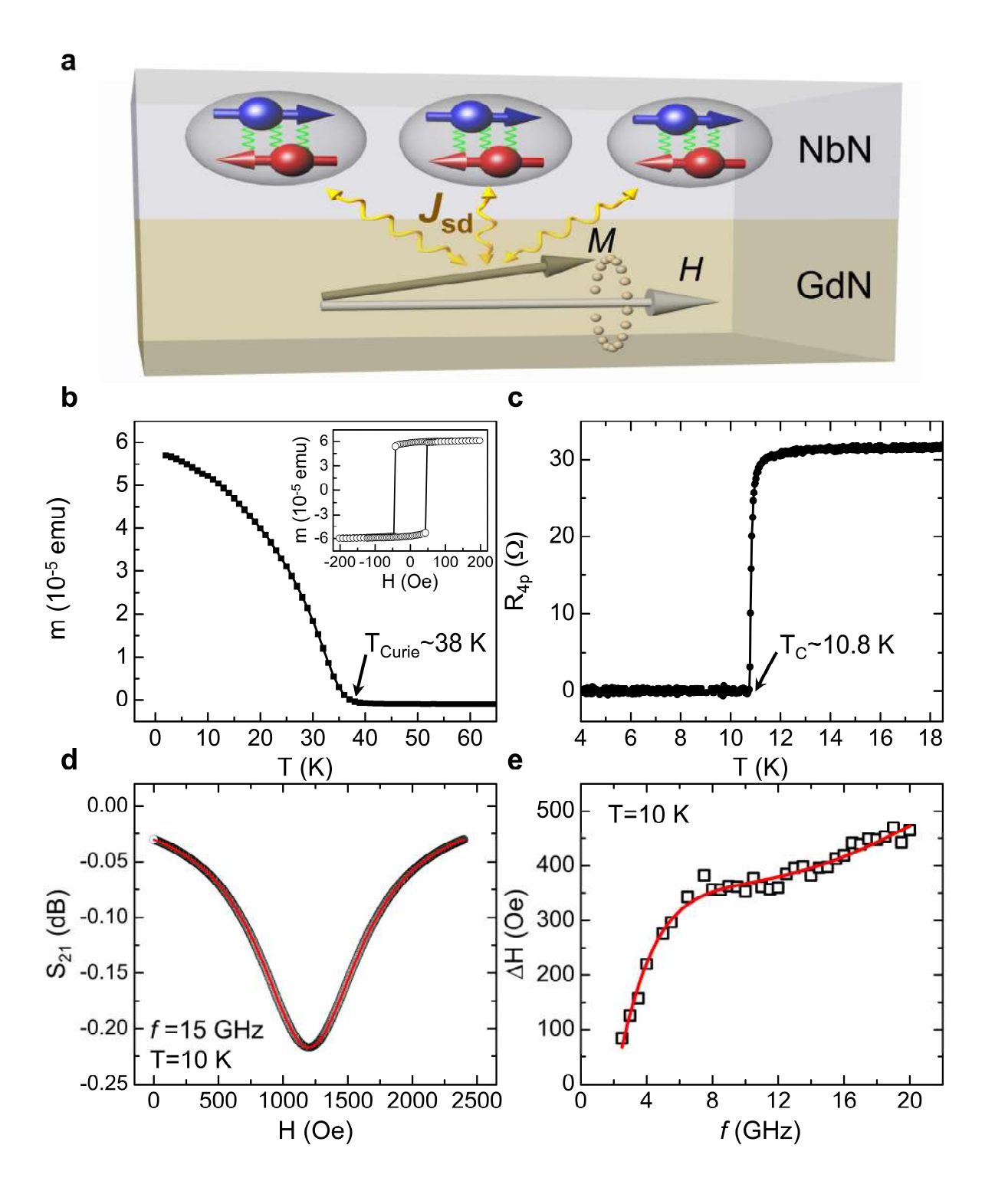


Figure 1 | Spin pumping into the SC NbN thin films. a, Schematic of the s-d exchange interaction (J_{sd}) between the spins in the Cooper pair in NbN layer and the rotating magnetization

of GdN layer under the ferromagnetic resonance conditions. **b**, The magnetic moment as a function of the temperature. Inset: The magnetic hysteresis loop at 5 K. **c**, The four-probe resistance as a function of the temperature. **d**, The typical ferromagnetic resonance spectrum measured at 10 K and under the RF frequency of 15 GHz. The red line indicates the Lorentz fitting curve to obtain the half linewidth based on equation (1). **e**, The half linewidths as a function of the resonance frequency at 10K. The red solid line is the fitting curve based on spin relaxation model. The results in Fig. 1b-1d are obtained on the NbN (10)/GdN (5)/NbN (10) sample.

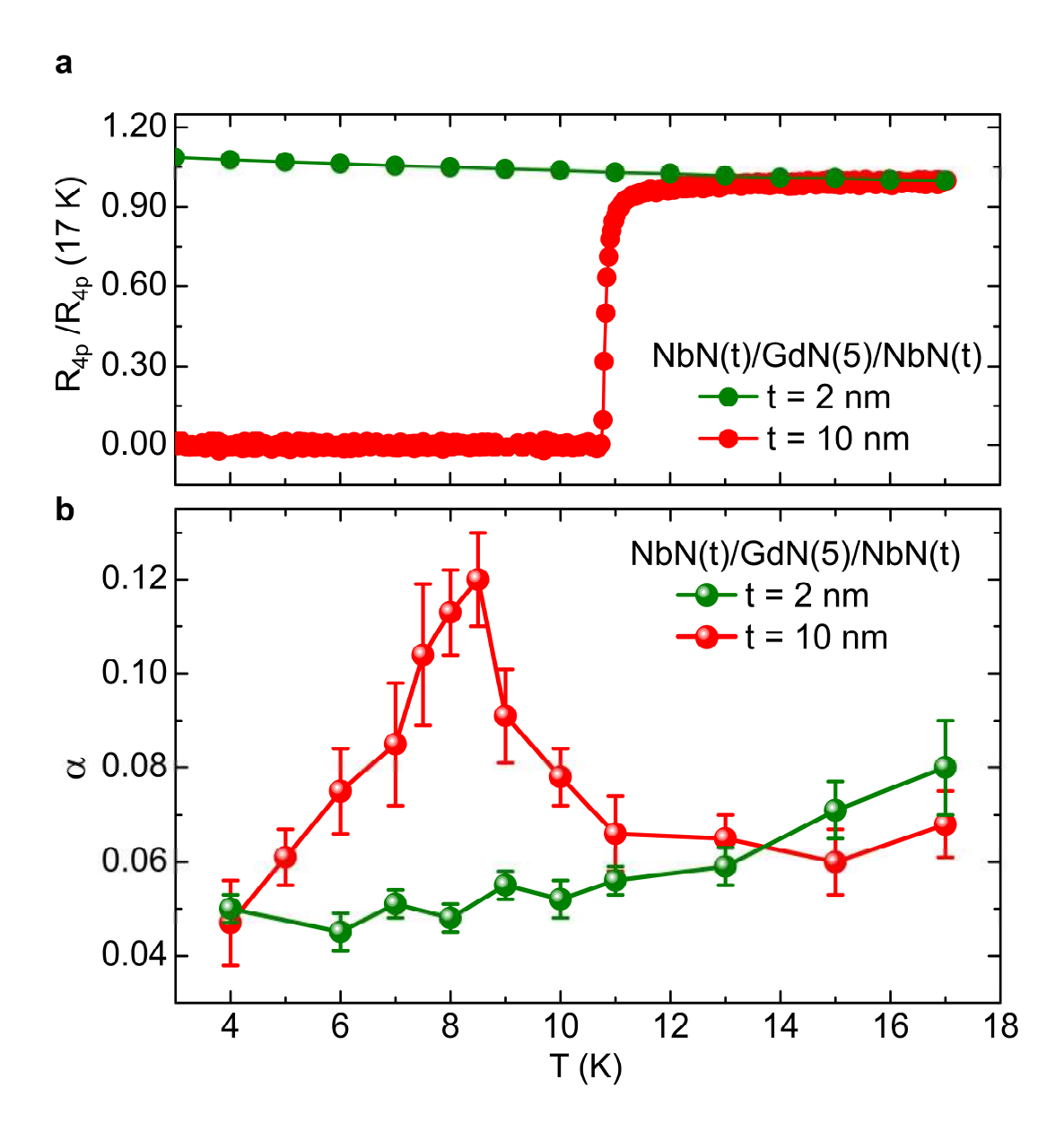


Figure 2 | **Spin dynamics of the SC NbN thin films probed via Gilbert damping. a,** The normalized four-probe resistance as a function of the temperature for the samples of NbN (2)/GdN (5)/NbN (2) and NbN (10)/GdN (5)/NbN (10), respectively. **b,** The Gilbert damping constant as a function of the temperature for the samples of NbN (2)/GdN (5)/NbN (2) and NbN (10)/GdN (5)/NbN (10), respectively.

Figure 3

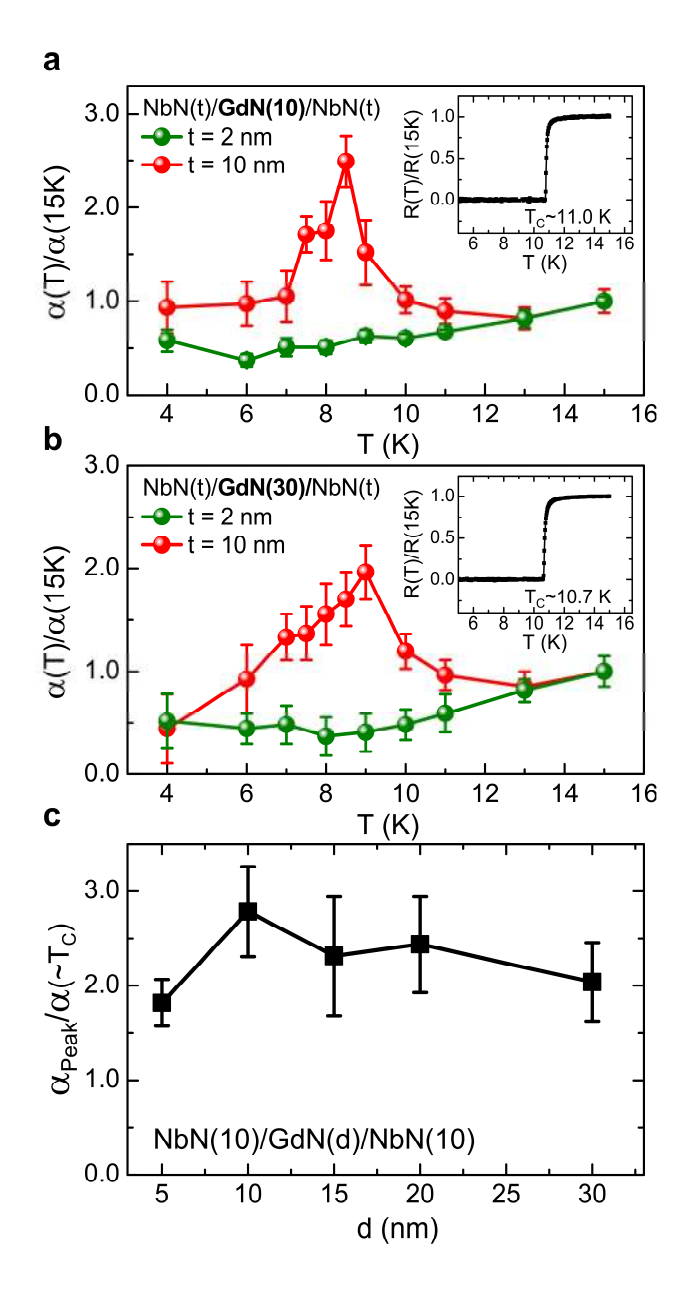


Figure 3 | **The GdN thickness effect on spin dynamics of the SC NbN thin films. a-b,** The Gilbert damping constant as a function of the temperature for the samples of NbN (2 or 10)/GdN (10)/NbN (2 or 10), and NbN (2 or 10)/GdN (30)/NbN (2 or 10). Insets of **a, b**: The normalized four-probe resistance as a function of the temperature for the samples of NbN (10)/GdN (10)/NbN (10) and NbN (10)/GdN (30)/NbN (10). **c,** The coherence peak height of the Gilbert damping as a function of the GdN layer thickness.



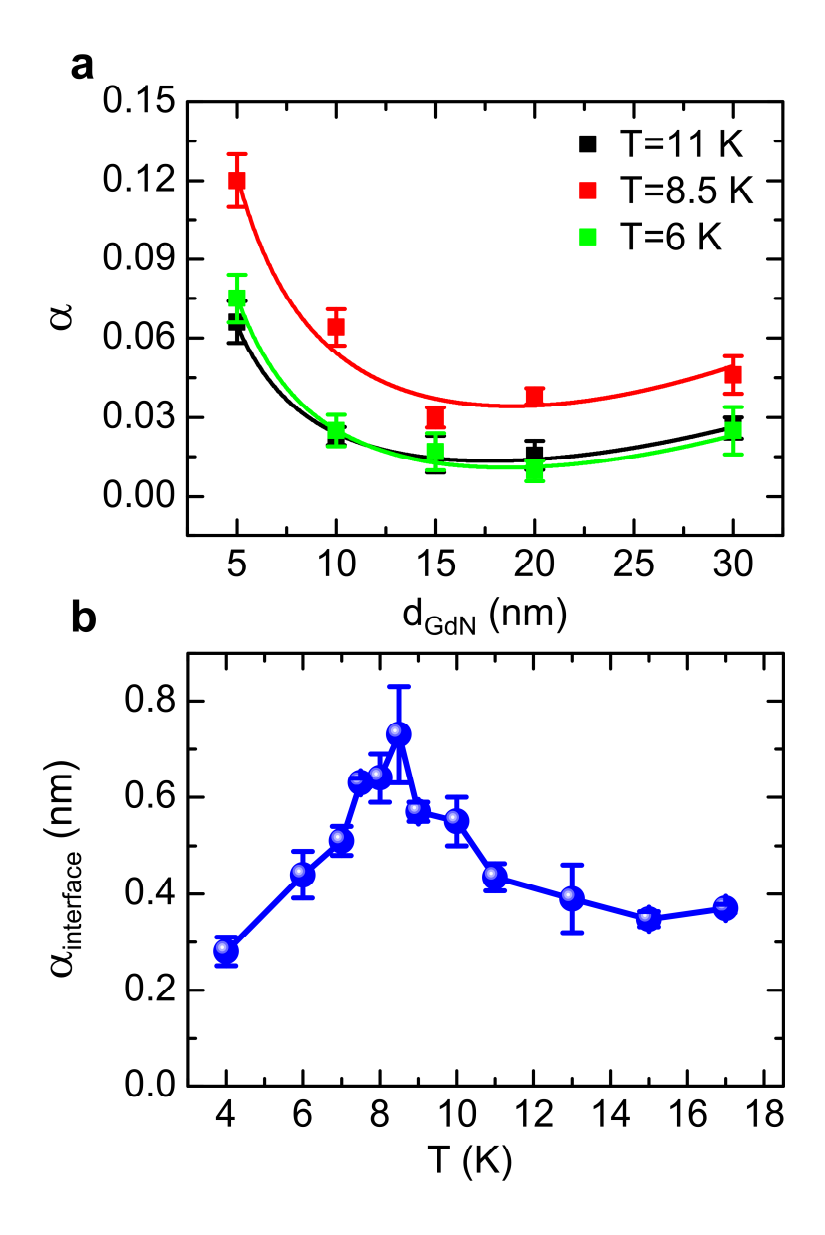


Figure 4 | **The interface-induced Gilbert damping at the NbN/GdN interface. a,** The Gilbert damping constant as a function of the GdN thickness for the samples of NbN (10)/GdN (d)/NbN (10) at T= 11 K, 8.5 K, and 6 K. **b,** The interface-induced Gilbert damping in the samples of NbN (10)/GdN (d)/NbN (10) as a function of temperature.